

## NEW TECHNOLOGY FOR HIGH DISINFECTION LEVEL OF FLEXIBLE ENDOSCOPES

Christophe Nicolet, François Avellan  
Laboratory for Hydraulic Machines  
EPFL Swiss Federal Institute of Technology  
Lausanne  
[christophe.nicolet@epfl.ch](mailto:christophe.nicolet@epfl.ch)  
[francois.avellan@epfl.ch](mailto:francois.avellan@epfl.ch)

Jordi Rossell  
Meditecnic SA  
14, Quai du Seujet  
CH-1201 Geneva  
[info@meditecnic.com](mailto:info@meditecnic.com)

### ABSTRACT

Maybe, one of the most promising applications of cavitation in the biomedical field is related to the cleaning and disinfecting capability of cavitation phenomenon. Recently, a new technology has been developed and patented for cleaning and high level disinfection of medical flexible endoscopes, which are acknowledged as one of the cause of hospital acquired infections, as called nosocomial infections. In the paper, the principle of operation of the equipment as well as the results of the experimental and numerical studies carried out at the EPFL Laboratory for Hydraulic Machines are presented. In this equipment, the cavitation process is achieved through the rapid shut-off of the flow by a rotating valve which leads the liquid to series of pressure and relief waves of controlled amplitude and phase. The liquid is then subjected to rapid changes of pressure, leading to the onset and the collapse of bubbles. The shock waves and the high shear stress during the bubble collapse strongly affects the cellular structure of the bio-organisms infecting the endoscope walls and notably the internal passages. Moreover, a continuous flow through the endoscope thoroughly eliminates the contaminant and impurities, processed by the cavitation phenomenon. Finally the high level of disinfection efficiency of the new technology is demonstrated through biological tests carried out with the original equipment.

### INTRODUCTION

The use of cavitation for medical cleansing purposes stems from Detaille [1], [2]. It was first used in the field of endodontics for the cleansing of tooth root-canal. A machine was developed and successfully tested by Lussi [3], [4]. Lussi has demonstrated the high efficiency of the cavitating process and patented the machine. This technique has demonstrated in this application its capability to extract biological debris from thin canals. Meditecnic SA further developed a new cavitation generation process, allowing achieving the same phenomena at bigger scale. As a result, new applications appeared to be within reached, i.e. contact lenses cleaning, catheters unclogging and flexible endoscopes cleaning and disinfection. This process was patented in 2003 (EP 1 146 914 B1). A commercial version dedicated for endoscope cleaning has been launched under the name

"Meditecnic<sup>Switzerland</sup> ST-02". This machine is able to eliminate all dirt from both the external surfaces and internal canals of an endoscope, see Fig. 1. The internal flow within the endoscope is subject to shut-of induced by a rotating valve, generating pressure fluctuations. This leads to the onset and the collapse of bubbles. The shock waves and the high shear stress occurring during the bubble collapse strongly affect the cellular structure of the bio-organisms trapped in the endoscope canals and notably the internal passages. Surgery endoscopes are equipped with different canals in the distal part (3) for air/water injection, surgery instruments passages and biopsy purposes.

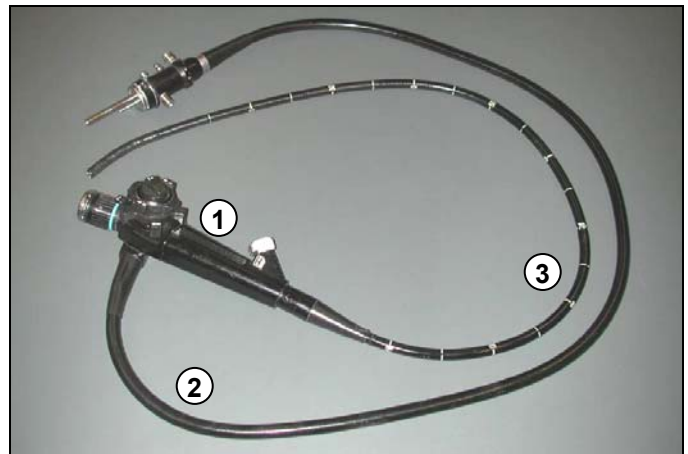


Fig. 1 Flexible endoscope made of: (1) handle, (2) instrumentation canal and (3) distal tube.

This paper describes first the principle of operation of the Meditecnic<sup>Switzerland</sup> ST-02. Then the machine test-rig which is fully instrumented is presented. The patterns of the internal flow of an endoscope during operation, the external flow being neglected, are characterized. The measurements of pressure fluctuations for different valve rotation frequency and endoscope box pressure level are performed and discussed. Based on the experimental results, a numerical modeling of the system is completed for the determination of eigen frequencies. Using flow visualization, different phase of bubble grow-up and collapse are evidenced. Finally, biological tests are presented

demonstrating the high level of cleaning and disinfection provided by this cavitating process.

## NOMENCLATURE

Definition	Symbol	Unit
Area of the Flow Passage Cross Section	$A$	$[m^2]$
Discharge	$Q$	$[m^3s^{-1}]$
Piezometric head	$H = z + \frac{p}{\rho \cdot g}$	$[m]$
Elevation	$z$	$[m]$
Hydraulic impedance	$Z$	$[sm^{-2}]$
Density	$\rho$	$[kgm^{-3}]$
Static Pressure	$p$	$[Pa]$
Atmospheric Pressure	$p_{atm}$	$[Pa]$
Vapor Pressure	$p_v$	$[Pa]$
Wave Speed	$a$	$[ms^{-1}]$
Local Friction Coefficient	$\lambda$	$[-]$
Pipe Diameter	$D$	$[m]$
Hydraulic Resistance	$R = \frac{\lambda \cdot dx \cdot  Q }{2 \cdot g \cdot D \cdot A^2}$	$[sm^{-2}]$
Hydraulic Inductance	$L_h = \frac{dx}{g \cdot A}$	$[s^2m^{-2}]$
Hydraulic Capacitance	$C = \frac{g \cdot A \cdot dx}{a^2}$	$[m^2]$
Pipe Length	$L$	$[m]$
Elementary Length	$dx$	$[m]$
Valve Rotation Frequency	$f_v = \frac{1}{T_v}$	$[Hz]$

## PRINCIPLE OF OPERATION

The cleaning process of a flexible endoscope with the Meditecnic<sup>Switzerland</sup> ST-02 starts by inserting the endoscope in the PMMA case (1), Fig. 2, filled with an appropriate solution. The mean pressure in the endoscope case is kept constant at 850 hPa, absolute, 200 hPa in the vacuum tank. Therefore, the fluid is forced to flow trough the internal canals of the endoscope up to the handle (2). The handle is connected to a rotating valve (4) by flexible PTFE pipes (3). The rotating valve switches alternatively between the endoscope tubing to the vacuum tank and the atmosphere (5). When connected to the vacuum tank the discharge is positive, whereas a little amount of air is trapped in the pipe (3) when the endoscope is connected to the atmosphere. The valve rotation generates periodic pressure wave trains inside the whole piping system made of the connecting pipes and the endoscope internal canals. These pressure waves induces bubbles grow up and collapse within the low pressure part of the piping, i.e. the endoscope internal canals. The combination of rapid pressure changes and bubbles collapse constitutes the fundamental active principle of the cleaning process. Disinfectant agents are added to prevent any bio-hazard according to the rules concerning medical cleaning devices. Therefore, the full cycle of disinfection comprises 3

sequences: 2 sequences of cleaning with a water/tri-enzymatic solution and one high-level disinfection sequence with water/peracetic acid (750 ppm). Each sequence is followed by a rinse phase. The full cycle lasts 30 minutes.

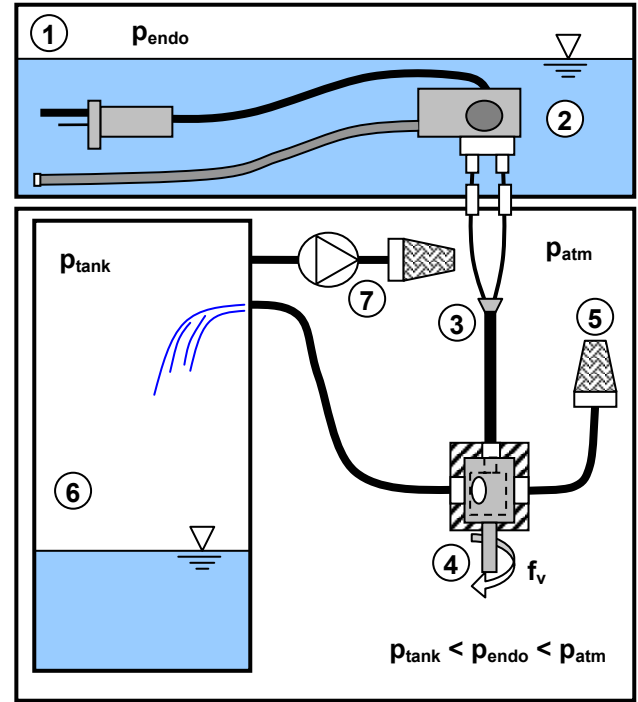


Fig. 2 Meditecnic<sup>Switzerland</sup> ST-02 system overview: (1) Endoscope case at 850 hPa filled with water and 0.7 % of peracetic acid; (2) Endoscope handle; (3) 3 mm and 8 mm inner diameter PTFE pipes connected through a trifurcation to (4), the rotating valve; (5) Connection to atmosphere at  $p_{atm}$ ; (6) Vacuum tank at 200 hPa; (7) Vacuum pump.

## EXPERIMENTAL SET-UP

For studying the dynamics of the cleaning process of the machine, an experimental set up is developed, see Fig. 3. A commercially available flexible endoscope is disassembled to have access to the different internal conduits.

The investigations are focused on pressure time history and bubbles grow up and collapse in the endoscope canal. Therefore, the endoscope and the PTFE connecting pipes are instrumented with 5 pressure transducers from the intake of the biopsy canal up to the rotating valve. The endoscope is placed in a tank (1), connected to a vacuum pump (7). The water level and the pressure inside the tank (1) remain constant by using a water intake (8) which compensates the outgoing discharge. To have access to the S5 and S4 transducers, the instrumented part of the biopsy canal (9), is successively brought outside and inside of the tank, Fig. 4. The PTFE pipes (3) are instrumented with the S1 to S3 transducers. The characteristics of the pressure instrumentation are summarized Table 1.

Pressure transducer	S1,S2,S3,S5	S4
Type	Kistler® 601A	Unisensor® Ceramic
Pressure	Dynamic	Absolute
LP-Filter	5 kHz	7.2 kHz
Sampl. Freq.	20 kHz	20 kHz
Samples	32'768	32'768
Mounting Material	Brass	PMMA
Pipe Inner Diameter	S1/S2: 8 mm S3/S5: 3 mm	3 mm

Table 1 Pressure instrumentation characteristics.

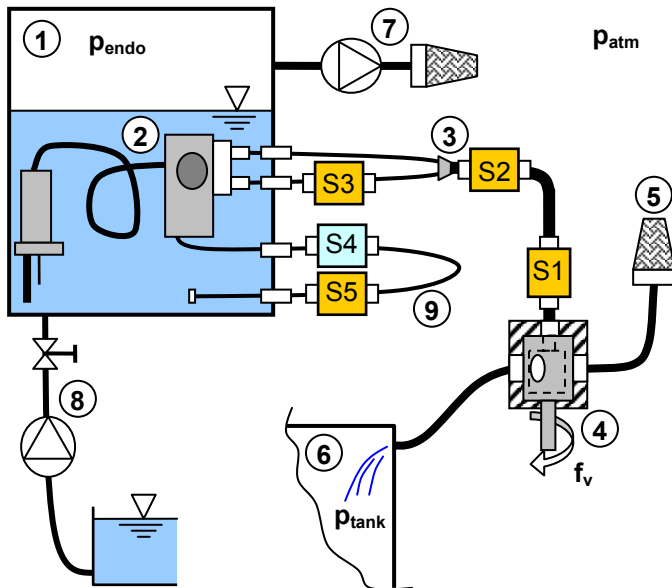


Fig. 3 Experimental setup overview with the S1 to S5 pressure transducers: (1) water filled tank at  $p_{\text{endo}}$ ; (2) Endoscope handle; (3) 3 mm and 8 mm inner diameter PTFE pipes connected through a trifurcation to (4), the rotating valve; (5) Connection to atmosphere at  $p_{\text{atm}}$ ; (6) Vacuum tank at 200 hPa; (7) Vacuum pump; (8) water intake; (9) biopsy canal.

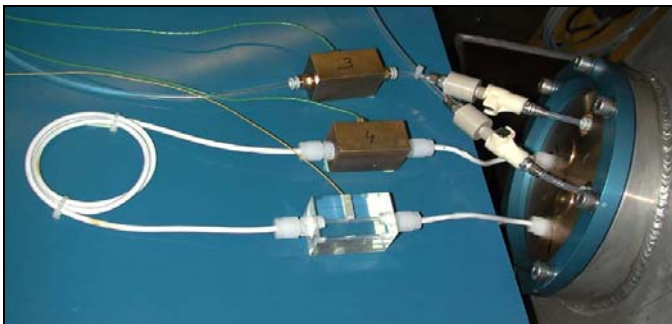


Fig. 4 Pressure transducers installed on the biopsy canal and the connecting pipe.

To carry out flow visualization in the biopsy canal, the canal of interest, a Unisensor® pressure transducer, Fig. 5, is embedded in a transparent body made of PMMA. The sensitive part of the transducer is shaped to fit exactly the biopsy canal of 3 mm inner diameter for minimizing the flow perturbations and providing a good access to the camera.

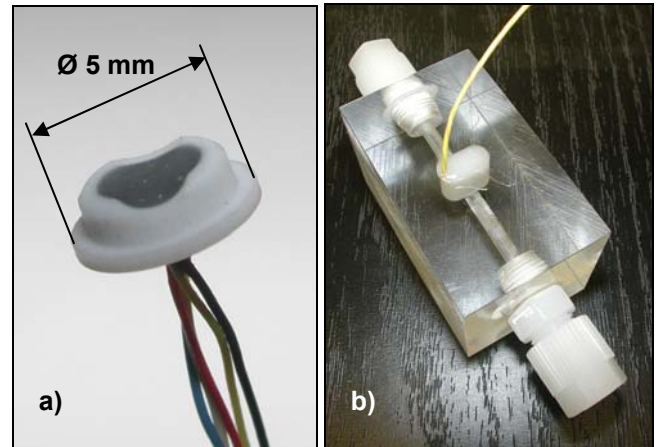


Fig. 5 Pressure transducer Unisensor® a) and its Plexiglas mounting b).

The static calibration curve of pressure transducer Unisensor® is presented Fig. 6. The dynamic response of these pressure transducers using the same piezo-resistive technology have already exhibited a frequency range extending up to 25 kHz, [5]. However a 7.2 kHz low pass filter is used for this transducer, see Table 1.

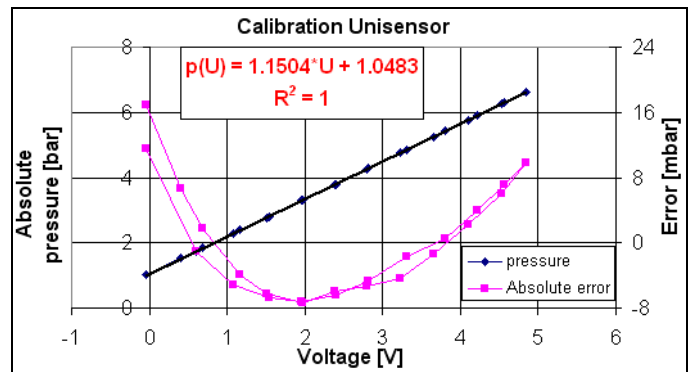


Fig. 6 Static calibration curve of the pressure transducer S4 .

The characteristic lengths of all the parts of the piping system equipped with the transducers are listed Fig. 7.

For the present study, only fresh water is used without acid peracetic or tri-enzymatic and the water is at the room temperature, i.e. 23°C.

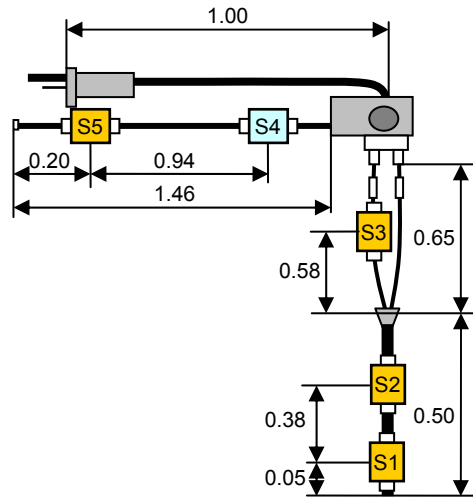


Fig. 7 Characteristic lengths of the piping system.

## PRESSURE FLUCTUATIONS

The pressure waves are generated by a rapid shut off of the flow. Depending on the characteristic times of the piping system and the discharge forced through the endoscope by the pressure difference between the endoscope case and the vacuum tank, the frequency and the amplitudes of the pressure waves are related to the 2 following parameters:

- the valve rotation frequency;
- the pressure level in the endoscope tank  $p_{\text{endo}}$ .

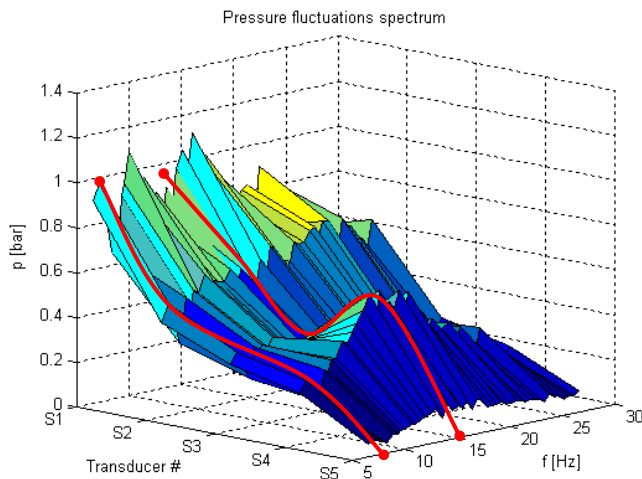


Fig. 8 Spectral representation of the pressure fluctuations at the locations #1 to #5 for  $p_{\text{endo}} = 850$  hPa.

First, the pressure fluctuations are measured for different valve rotation frequencies by keeping constant  $p_{\text{endo}}$  at 850 hPa. The range of frequency values extends from 5.5 Hz to 26.5 Hz for every 0.5 Hz. For each excited frequency  $f_i$ , the amplitude of the corresponding pressure fluctuations  $|p(f_i)|$  is extracted by Fast Fourier Transform. This is completed for each transducer S1 to S5. The pressure fluctuation spectrum obtained is represented as a function of the different pressure transducers and the excited frequency  $f_i$ , see Fig. 8.

First, the effect of the boundary conditions can be noticed at the intake of the biopsy canal, transducer S5, where a condition of constant pressure is imposed. Moreover, the spectrum of the pressure fluctuations shows 2 dominant waves of 7.5 Hz and 15 Hz frequencies. The wave corresponding to the 15 Hz frequency gives the maximum amplitudes for the biopsy canal, which can be considered as a suitable effect for cleaning and disinfection.

Thus, the influence of the pressure level  $p_{\text{endo}}$  in the endoscope tank is investigated for a 15 Hz valve rotation frequency. For this frequency,  $p_{\text{endo}}$  is set for 850, 750 and 650 hPa. Since the pressure signal data sampling is synchronized with valve revolution, the signal are phase averaged over a complete valve revolution, see Fig. 9 to Fig. 11. The pressure at the rotating valve location is also represented with the value of  $p_{\text{tank}} = 200$  hPa over half of one valve revolution and the atmospheric pressure for the other half.

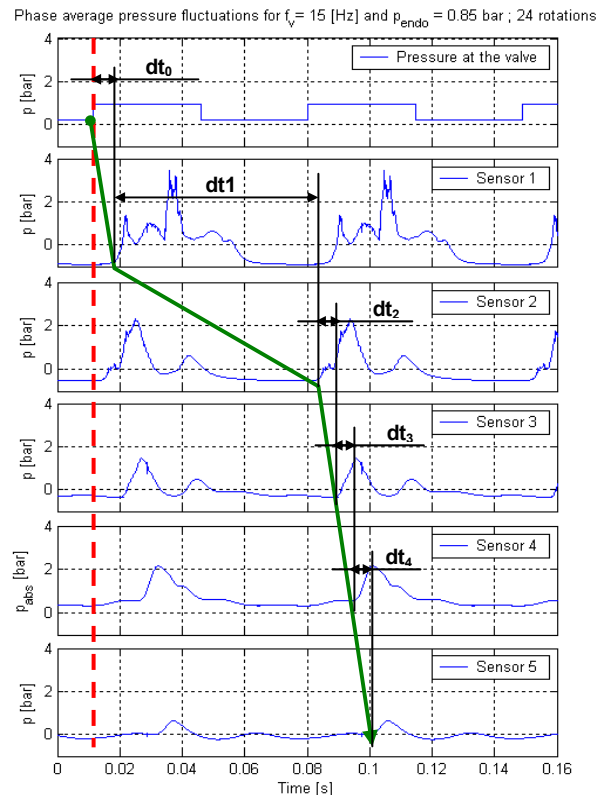
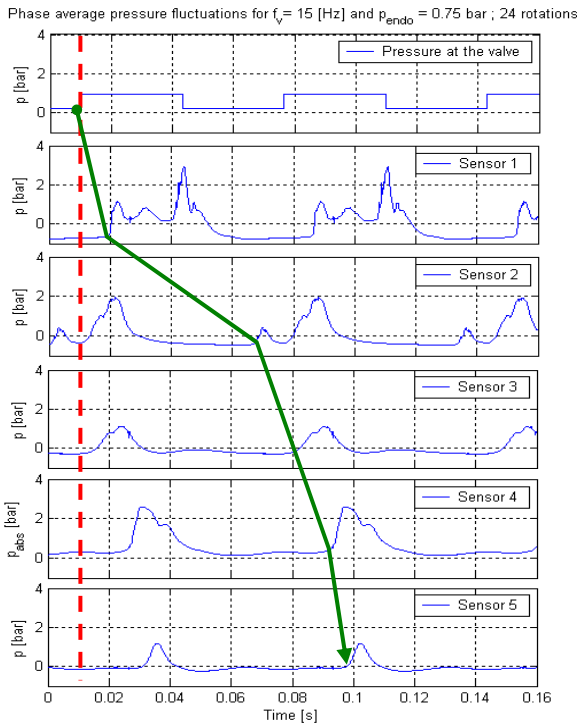


Fig. 9 Phase average pressure fluctuations for  $p_{\text{endo}} = 850$  hPa.

On Fig. 9 to Fig. 11 the pressure wave, identified as the sudden increase of pressure, can be followed in the piping system, solid green line. The wave starts at the time when the rotating valve connect the endoscope to  $p_{\text{tank}}$ , marked by the red dashed line, and travel all along the biopsy canal up to the intake. First, the amplitudes of the pressure wave decrease all along the piping system and especially between the pressure transducer S2 and S3. It corresponds to the contraction and losses effects of the trifurcation where a part of the wave is reflected. However, the pressure fluctuation amplitudes at the pressure transducer S4 are higher than at the one at pressure

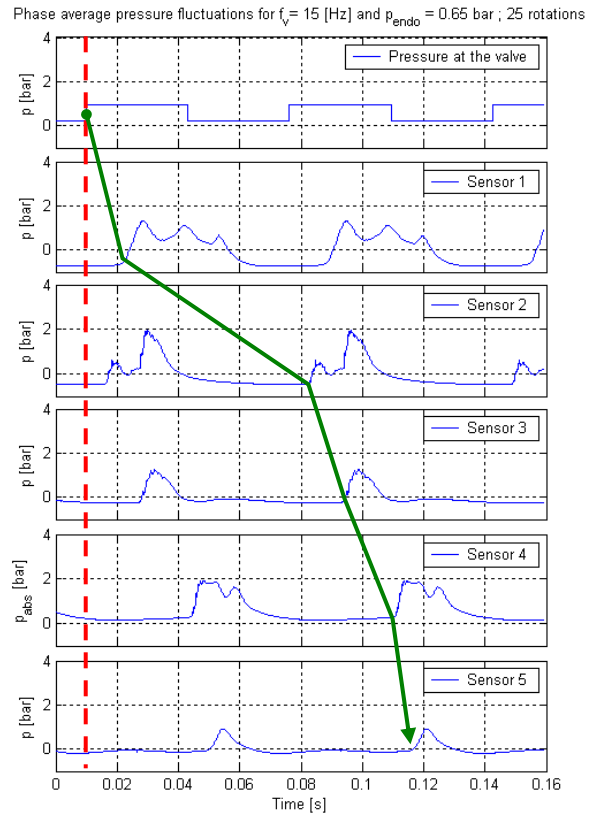
transducers S3 and S5, according to the spectrum of Fig. 8. Moreover, it can be noticed that the minimum of pressure measured at pressure transducer S4 decreases with the pressure  $p_{\text{endo}}$ .



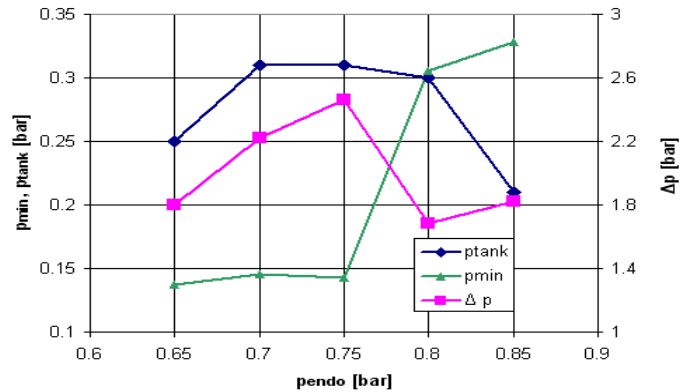
**Fig. 10** Phase average pressure fluctuations for  $p_{\text{endo}} = 750$  hPa.

Fig. 12 summarizes for the pressure transducer S4 the minimum of pressure  $p_{\text{min}}$ , the amplitudes of pressure fluctuations peak-to-peak  $\Delta p$  and pressure level in the tank  $p_{\text{tank}}$ . The minimum of pressure at pressure transducer S4 is for  $p_{\text{endo}} = 650$  hPa with  $p_{\text{min}} = 140$  hPa. This pressure does not reach the vapor pressure, which is equal to 28 hPa at 23°C temperature. Moreover, this operating condition is not stable because of the small pressure difference between the tank and the endoscope. The maximum of pressure pulsation is obtained for  $p_{\text{endo}} = 700$  hPa bar and corresponds to  $\Delta p = 0.25$  MPa.

By following the pressure wave propagation in the system on Fig. 9 to Fig. 11, the time interval is determined between 2 transducers. Knowing the distance between those transducers from Fig. 7, the mean wave speed is determined for the corresponding interval. The resulting wave speed values are reported Fig. 13 for the 4 intervals and for the 3 endoscope pressure conditions  $p_{\text{endo}}$ .



**Fig. 11** Phase average pressure fluctuations for  $p_{\text{endo}} = 850$  hPa.



**Fig. 12** Minimum of absolute pressure  $p_{\text{min}}$ , pressure of the tank  $p_{\text{tank}}$  and peak-to-peak pressure  $\Delta p$  at the pressure transducer S4 as a function of the pressure at the endoscope  $p_{\text{endo}}$ . Rotational frequency is equal to 15 Hz.

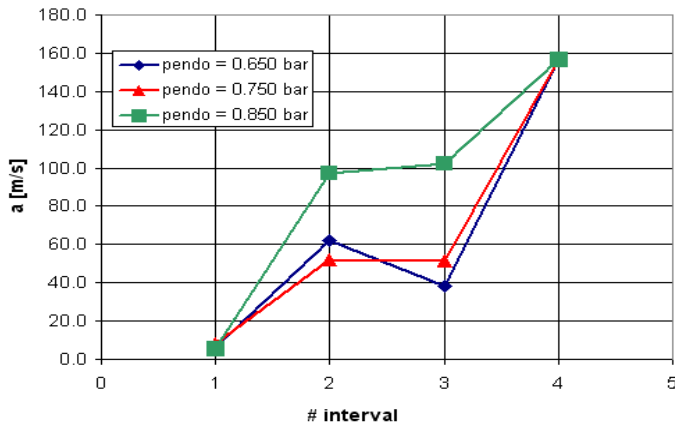


Fig. 13 Mean wave speed for the 4 intervals for  $p_{\text{endo}} = 0.85$ , 0.75 and 0.65 bar. Rotational frequency is equal to 15 Hz

The mean wave speed in the intervals decreases as the interval is closer to the rotating valve. This is due to the decrease of the mean pressure along the pipes from the intake of the biopsy canal until the rotating valve. As a result, the bubbles growing up and collapsing in the pipes are larger at the valve than at the biopsy canal intake. The mean wave speed in the pipes is strongly dependent on the void fraction as noticed in [6]. Unless the amount of bubbles increases when  $p_{\text{endo}}$  decreases, the wave speed of interval 4 does not change significantly. It also means, that there is only a small amount of bubbles in the interval 4, biopsy canal. On the other hand, the wave speed at interval 1 does not change because the amount of bubbles is high for the 3 pressure conditions. Whereas, the wave speed of the intervals 2 and 3 is strongly affected by the decrease of  $p_{\text{endo}}$  from 0.85 bar to 0.75 bar.

Using the mean wave speed at  $p = 850$  hPa presented Fig. 13, and the pipes length of Fig. 7, a hydroacoustic model of the system is established. The impedance method modeling is based on the analogy between wave propagation in pipes and electrical lines according to [7]. The hydraulic impedance of the system is computed using the direct impedance method described by [8]. The whole impedance of the system is defined as:

$$\underline{Z}(j\omega) = \frac{\underline{H}(j\omega)}{\underline{Q}(j\omega)}$$

The corresponding impedance for the circuit is displayed Fig. 15. It makes visible:

- the eigen frequencies of the system as seen by the rotating valve corresponding to  $x = 0$ ;
- the locations, for a given frequency, of the minima and maxima of the eigen mode shapes of the system given by the impedance along  $x$ .

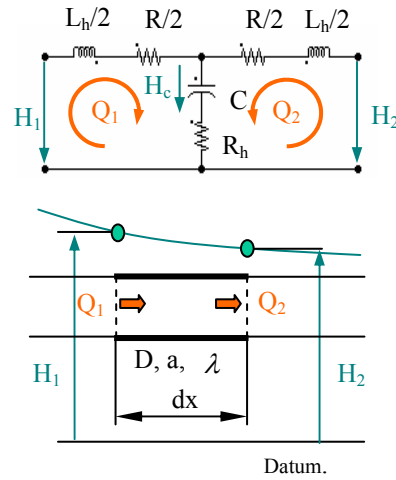


Fig. 14 Electrical analogy between an electrical line and a hydraulic pipe.

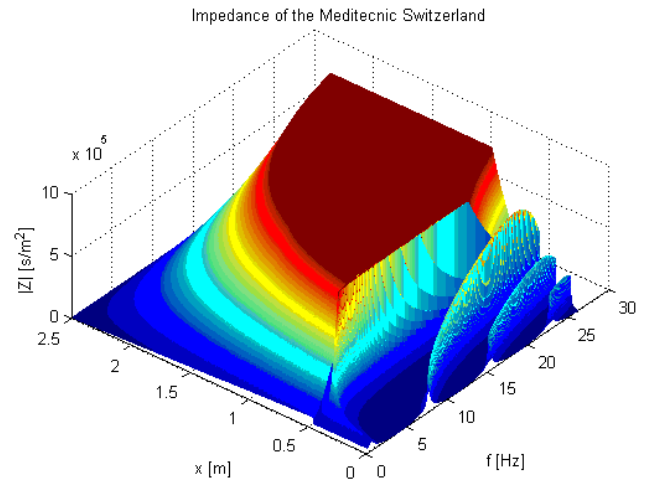


Fig. 15 Impedance of the Meditecnic<sup>Switzerland</sup> ST-02 calculated from  $x = 0$  (at the valve) until  $x = 2.5$  m (end of the biopsy canal where  $|Z| = 0$ ) as a function of the frequency.

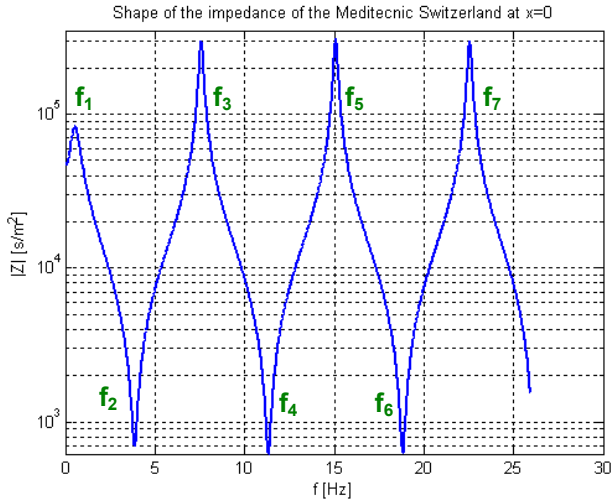


Fig. 16 Eigen frequency of the system as seen by the rotating valve.

The impedance of the circuit at  $x = 0$  shows eigen frequencies at 0.7 Hz, 4 Hz, 7.6 Hz, 11.5 Hz, 15 Hz, 18.5 Hz and 22.5 Hz, see Fig. 16. These frequency values confirm that the 2 modes shape of Fig. 8 correspond to 2 eigen frequencies of the system excited by the valve rotation.

Fig. 17 and Fig. 18, the minima and maxima of pressure of the eigen mode shape for  $f_v = 7.6$  Hz and  $f_v = 15$  Hz correspond to the minima and maxima of impedance. Respectively minima and maxima of impedance correspond to maxima and minima of discharge.

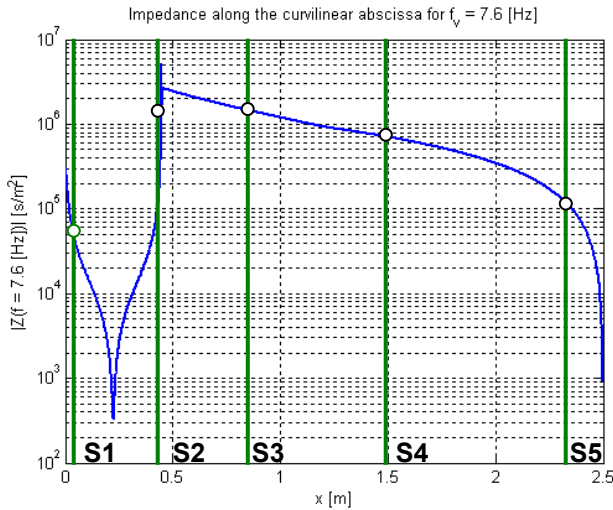


Fig. 17 Impedance along the curvilinear abscissa for the eigen mode at  $f_v = 7.6$  Hz.

The shape of the eigen mode at  $f_v = 7.6$  Hz shows good agreements with the measurements. However, if the shape of the eigen frequency  $f_v = 15$  Hz is similar to the measurements, the location of the maxima does not show a good agreement. This is mainly due to a limitation of the hydroacoustic model in use which assumes a constant wave speed for inch interval. However in the real system, the wave speed constantly changes

from the biopsy canal intake up to the rotating valve according to the local void fraction distribution.

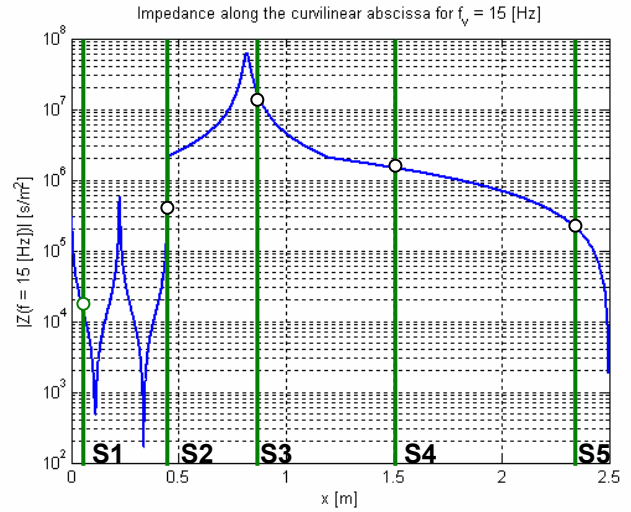


Fig. 18 Impedance along the curvilinear abscissa for the eigen mode at  $f_v = 15$  Hz.

### FLOW VISUALIZATIONS

For the visualization of the bubbles appearing in the biopsy canal, the strobe flash is synchronized with the S4 up-front pressure signal. A time lag is then introduced for capturing the shape of the bubbles at different stages over a given valve rotation time period. The following time lags are selected for the visualizations:

$$\frac{t_r}{T_v} = 73\% ; 97\% ; 100\% ; 103\%$$

The pressure in the endoscope tank corresponds to  $p_{\text{endo}} = 700$  hPa for all the visualizations. Typical pair of photographs corresponding to the above mentioned time lag are presented Fig. 19 to Fig. 22. The following observations can be drawn for:

- $t_r = .73T_v$  the pressure minimum is reached and the bubbles are visible, their diameter being half the pipe inner diameter.
- $t_r = .97T_v$ , the pressure is slightly higher than the minimum value but the bubble diameters remains the same as for  $t_r = .73T_v$ .
- $t_r = T_v$ , the pressure is increasing rapidly and the larger bubbles collapse or break into bubble of smaller diameters.
- $t_r = 1.03T_v$ , the pressure is at the highest value and bubbles are no longer visible.

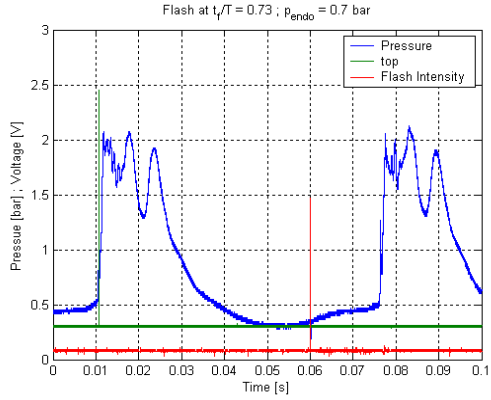
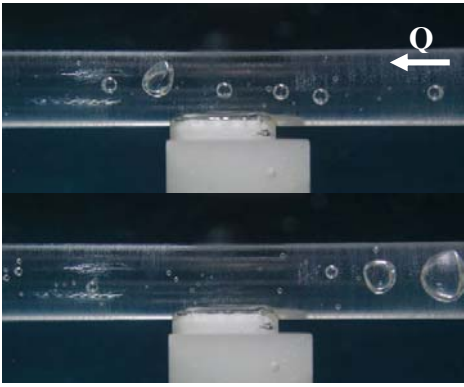


Fig. 19 Bubbly flow for  $p_{\text{endo}} = 700$  hPa and  $t_f = .73T_v$ .

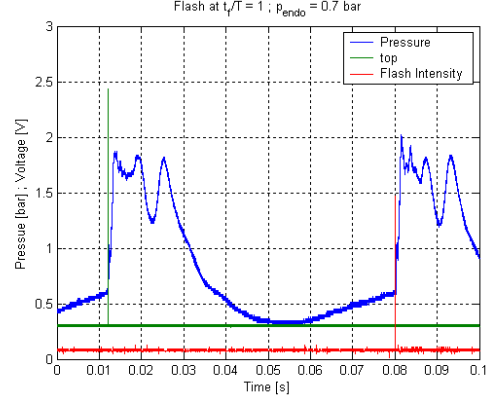
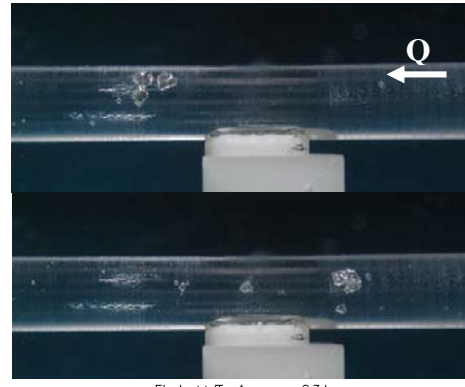


Fig. 21 Bubbly flow for  $p_{\text{endo}} = 700$  hPa and  $t_f = T_v$ .

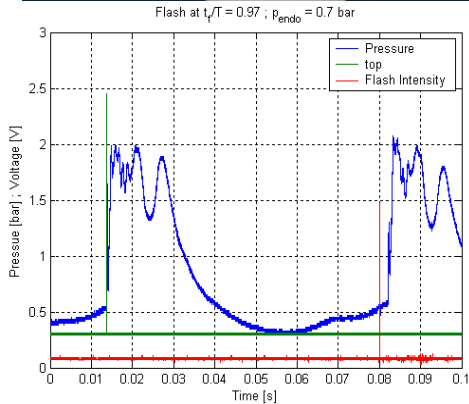
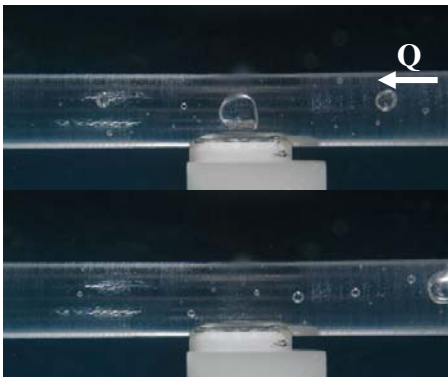


Fig. 20 Bubbly flow  $p_{\text{endo}} = 700$  hPa and  $t_f = .97T_v$ .

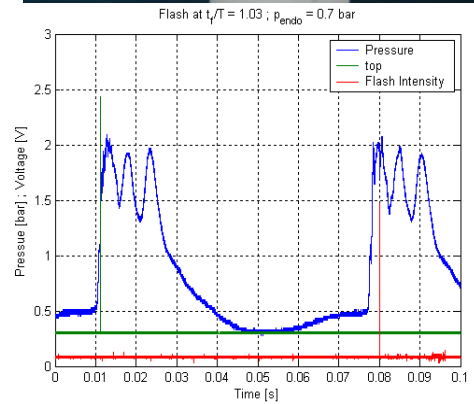
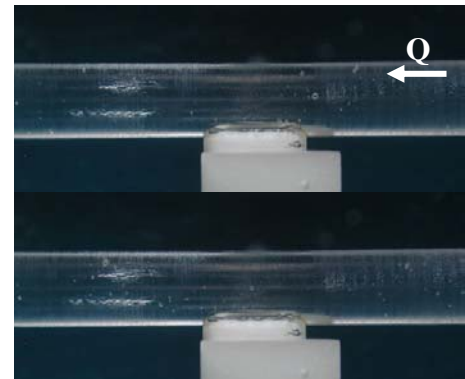


Fig. 22 Bubbly flow  $p_{\text{endo}} = 700$  hPa and  $t_f = 1.03T_v$ .



## CLEANING & DISINFECTION TESTS

The cleaning and disinfection tests are carried by injecting solution of known organism contamination within the endoscope. After subjecting this endoscope without any prewashing to the cleaning and disinfection process of the Meditecnic<sup>Switzerland</sup> ST-02, recoveries of organisms are made from each canal according to a standard methodology to discover any survivors. Contamination controls are assessed to measure the logarithmic reduction between the initial contamination and the one recovered from the endoscope canals. The tests results are presented Table 2. The tests carried out on the Meditecnic<sup>Switzerland</sup> ST-02 for each of the tested micro-organisms, comply with the values as requested according to the previous Biotech-Germande work [9], [10], [11].

Micro-organism tests	Average	Requested [9][10]
<b>Pseudomonas aeruginosa</b> CIP 103467	8.7 ± 0.1	7
<b>Aspergillus niger</b> ATCC 16404	6.5 ± 0.2	6
<b>Mycobacterium terrae</b> CIP104321	7.1 ± 0.2	5
<b>Bacillus subtilis</b> ATCC 9372	7.2 ± 0.8	4
<b>Bacillus cereus</b> CIP 78.3	6.8 ± 0.5	4

**Table 2** The average logarithmic reductions obtained with MeditecnicSwitzerland ST-02 without pre-washed, results from Biotech-Germande.

## CONCLUSIONS

The operating principle of a cleaning and disinfection system for flexible endoscopes is investigated. This system made of the internals canals of the endoscope, the PTFE connecting pipes and the rotating valve is subject to low pressure and pressure fluctuations. The flow visualizations demonstrate that the combination of those effects induce bubbles grow-up and collapse in the biopsy canal of the endoscope. However, the minimum of pressure in this canal is always above the vapor pressure, meaning that bubbles observed in the biopsy canal are trapped air and not vapor. Nevertheless, further developments are necessary to determine influence of both the temperature of 37°C and the solutions of tri-enzymatic detergent/peracetic acid on the cavitation occurrence in the Meditecnic<sup>Switzerland</sup> ST-02.

The air bubbles strongly affect the hydroacoustic characteristics of the system, and induce very low eigen frequencies which are in the frequency range of the rotating valve. Two eigen frequencies of the system, at 7.5 and 15 Hz, are identified experimentally and confirmed by an impedance calculation. This computation is based on the wave speed of the different pipes of the system identified experimentally. The eigen mode at 15 Hz induces high pressure fluctuations in the biopsy canal, which is a suitable effect.

Finally, the cleaning and disinfection tests demonstrate that the combination of pressure fluctuations, bubble collapse and peracetic acid give very good satisfaction.

## ACKNOWLEDGMENTS

This study was financially supported by Meditecnic SA and we want to thank sincerely Pierre-Alain Bionda and Julien Mathez from Meditecnic SA for their collaboration in the development phase. We thank gratefully Silvia Natal, Faïçal Guennoun and Dr. Mohamed Fährat from the EPFL-Laboratory for Hydraulic Machines their help in setting up the experimental work.

## REFERENCES

- [1] DETAILLE, L., Belgium Patent N° 821.274, 1974.
- [2] DETAILLE, L., Belgium Patent N° 834.432, 1976.
- [3] LUSSI, A., NUSSBACHER, U., GROSREY, J. et al. ; "A novel noninstrument technique for cleansing the root-canal system", *Journal of Endodontics*, vol. 19 N°11, Nov. 1993.
- [4] LUSSI, A., MESSERLI, L., HOTZ, P., GROSREY, J. ; "A new noninstrumental technique for cleaning and filling root canals", *Journal of Endodontics*, vol. 18, 1-6, 1995.
- [5] FARHAT, M. , NATAL, S. , AVELLAN, F. , PAQUET, F., LOWYS, P.-Y. , COUSTON, M. ; "Onboard Measurements of Pressure and Strain Fluctuations in a Model of low Head Francis Turbine. Part 1 : Instrumentation ". *Proceedings of the 21st IAHR Symposium on Hydraulic Machinery and Systems*, Lausanne, Switzerland, 9-12 September 2002, pp. 865-872.
- [6] WALLIS & GRAHAM; "One-dimensional two-phase flow", Mc Graw-Hill, 1969.
- [7] JAEGER, C., ; "Fluid transients in hydro-electric engineering practice". Glasgow: Blackie, 1977.
- [8] BLOMMAERT, G. , AVELLAN, F. , PRENAT, J.-E. , BOYER, A. ; "Evaluation de la stabilité d'installations hydroélectriques à partir d'essais sur modèle réduit : étude expérimentale ". *Colloque SHF : machines hydrauliques, instationnarités et effets associés*, Chatou, France, 21-22 novembre 2000.
- [9] RUTALA W., WEBER, D.; "FDA-Labeling requirements for disinfection of endoscopes: a counterpoint – infect control Hosp Epidemiol", 1995, 4, 231-35.
- [10] SPACH, D. H., SILVERSTEIN, F. E., STAMM, W. E. ; "Transmission of infection by gastrointestinal endoscopy and bronchoscopy". *Ann. Intern. Med.*, 1993, 2, 117-128.
- [11] LUU DUC, D., RIBIOLLET, A., DODE, X., DUCÉL, G., MARCHETTI, B., CALOP, J. ; "Evaluation of the microbicidal efficacy of Steris System I for digestive endoscopes using GERMANDE and ASTM validation protocols". *Journal of Hospital Infection*, vol 48, 135-141, 2001.